

First principles calculations on the high-pressure behavior of magnesite

LIDUNKA VOČADLO

Research School of Geological and Geophysical Sciences, Birkbeck College and University College London, Gower Street, London WC1E 6BT, U.K.

ABSTRACT

The equation of state and high pressure (>200 GPa) behavior of magnesite were investigated using first principles pseudopotential calculations based upon density functional theory within the generalized gradient approximation. Using a third-order Birch-Murnahan equation, the calculations predict a bulk modulus $K_T(0) = 99.0(5)$ GPa with a $\partial K/\partial P = 4.28(1)$; with a fixed $\partial K/\partial P = 4$, the $K_T(0)$ is 111(1) GPa. The results show very good agreement with recent experimental data. The simulations also confirm experimental studies which show that the CO_3 groups are rigid incompressible units while the Mg-O bond length undergoes significant compression. The fully relaxed calculations show no phase transition within this pressure range, and therefore magnesite may be stable throughout the lower mantle subject to temperature destabilization.

INTRODUCTION

Magnesite, MgCO_3 , is thought to be the only high pressure carbonate phase stable in the presence of silicates throughout the mantle (Eggler et al. 1976; Brey et al. 1983); it therefore could be the stable host for carbon in the Earth's mantle (Canil and Scarfe 1990; Biellmann et al. 1993; Redfern et al. 1993). However, despite several recent attempts to determine the high pressure behavior of magnesite, the experimentally determined equation of state and the high pressure crystallographic behavior of this phase differ between different groups. The isothermal bulk modulus of magnesite, $K_T(0)$, and its first-derivative with respect to pressure, $\partial K/\partial P$, have been determined in a number of studies; two similar results were obtained by Redfern et al. (1993) and Fiquet et al. (1994). Using a third-order Birch-Murnahan fit to experimental powder diffraction pressure-volume data, Redfern et al. (1993) determined a $K_T(0)$ of 142(9) GPa with $\partial K/\partial P$ fixed at 4, and a $K_T(0)$ of 151(7) GPa with a $\partial K/\partial P$ of 2.5; Fiquet et al. (1994) determined a $K_T(0)$ of 138(3) GPa with a $\partial K/\partial P$ fixed at 4, and a $K_T(0)$ of 156(4) GPa with a $\partial K/\partial P$ of 2.5(2). However, more recently, a third powder diffraction study (Zhang et al. 1997) and a single crystal diffraction study (Ross 1997) both obtained much lower values. Zhang et al. (1997) determined a $K_T(0)$ of 103(1) GPa with a $\partial K/\partial P$ fixed at 4, and a $K_T(0)$ of 108(3) GPa with a $\partial K/\partial P$ of 2.3, while Ross (1997) determined a $K_T(0)$ of 111(1) GPa with a $\partial K/\partial P$ fixed at 4, and a $K_T(0)$ of 117(3) GPa with a $\partial K/\partial P$ of 2.3(7). Furthermore, new powder diffraction data from Fiquet and Reynard (1998) gives a K_T of 115(1) with $\partial K/\partial P$ fixed at 4, and a $K_T(0)$ of 108(2) with a $\partial K/\partial P$ of 4.6(2). The later values are compatible with ultrasonic measurements for the adiabatic incompressibility of $K_S(0) = 112$ and 113.8

GPa (Christensen 1972; Humbert and Plicque 1972). In addition to the discrepancies in the experimental equation of state, a phase transition was suggested to occur around 25 GPa (Fiquet et al. 1994), although other groups have found no such transition (Gillet 1993; Williams et al. 1992; Katsura et al. 1991; Ross 1997) and more recent data (Fiquet and Reynard 1999) indicate that the observed phase transition may have been an artifact of the experiment. The high pressure behavior of magnesite merits further study, namely to determine theoretically the equation of state and phase stability of magnesite at the conditions that exist throughout the Earth's lower mantle. Computer simulations not only provide an alternative method by which to address these problems, but there is also the added advantage that they are not constrained by experimental limitations and therefore the entire pressure range required in order to study the lower mantle may be accessible.

In this paper, *ab initio* computer calculations have been performed on magnesite to very high pressures (>200 GPa). Anisotropic compression data and equation of state parameters are obtained from a third-order Birch-Murnahan fit to the compressional data and compared with previous experimental work.

SIMULATION TECHNIQUES

The pseudopotential method was used to calculate the high pressure behavior of magnesite. *Ab initio* density functional theory has been used, with the electronic exchange-correlation energy treated via the generalized gradient approximation (GGA), coupled with non-norm-conserving ultrasoft Vanderbilt pseudopotentials (Vanderbilt 1990) as implemented in the VASP code [Vienna *ab initio* simulation package (Kresse and Furthmüller 1996)]. These ultrasoft pseudopotentials have significantly smoother pseudo-wavefunctions which therefore require smaller basis sets and consequently this makes them highly efficient. With these pseudopotentials, calculations give results that are very close to, or indistinguishable from, the

*E-mail: l.vocadlo@ucl.ac.uk

best all-electron first principles methods currently available. Details of the construction of the pseudopotentials can be found in Kresse and Hafner (1994). The pseudopotential methodology has previously been shown to work well for high pressure simulations on a number of phases (Vocadlo et al. 1997; Vocadlo et al. 1999) and first principles calculations on silicate phases such as perovskite have been successful (Wentzcovitch et al. 1995); however, these are the first *ab initio* simulations on magnesite.

Fully relaxed computer calculations on the 30 atom MgCO_3 cell, relaxing both atomic positions and cell shape, were performed at nine volumes corresponding to a compression range up to >200 GPa. A 12 electronic k-point sampling grid in the irreducible wedge of the first Brillouin zone was used giving energy convergence to less than 0.005 eV/atom. Planewave cutoffs were chosen (400 eV) such that the energy convergence became less than 0.01eV/atom.

RESULTS

A third-order Birch-Murnaghan equation of state was fitted to the energy-volume data using the equation (see e.g., Poirier 1991):

$$E(V) = E_1 + E_2 + E_3$$

where

$$E_1 = \frac{9}{4} K_T(0) V_0 \left(\frac{V_0}{V} \right) \left[\frac{1}{2} \left(\frac{V_0}{V} \right)^{\frac{1}{3}} - \left(\frac{V}{V_0} \right)^{\frac{1}{3}} \right]$$

$$E_2 = \frac{9}{16} K_T(0) \left(\frac{\partial K}{\partial P} - 4 \right) V_0 \left(\frac{V_0}{V} \right) \left[\left(\frac{V_0}{V} \right) - 3 \left(\frac{V_0}{V} \right)^{\frac{1}{3}} + 3 \left(\frac{V}{V_0} \right)^{\frac{1}{3}} \right]$$

$$E_3 = E(V_0) - \frac{9}{16} K_T(0) V_0 \left(\frac{\partial K}{\partial P} - 6 \right)$$

V_0 is the volume at $P = 0$ and $E(V_0)$ is the corresponding internal energy. $K_T(0)$ is the isothermal bulk modulus, and $\partial K/\partial P$ its first derivative with respect to pressure. Fitting the E vs. V data to this equation gave a $K_T(0)$ of 99 GPa and a $\partial K/\partial P$ of 4.28 (Fig. 1). Incorporating these parameters into a third-order Birch-Murnaghan equation gives the pressure as a function of volume. The energy-volume-pressure data are shown in Table 1. Fixing $\partial K/\partial P = 4$, the energy-volume data gave a $K_T(0)$ of 111 GPa, although, as can be seen from Figure 1, the second order Birch-Murnaghan equation gives a poor fit to the $E(V)$ data and is not, therefore, used in the subsequent analysis. These results show good agreement with the most recent experiments and are summarized in Table 2.

One of the disadvantages of the use of GGA in the calculations is that although it predicts highly accurate structural and elastic properties, it overestimates the minimum energy volume of the system by ~3%. The simulations predict a V_0 of 287.49 \AA^3 compared to the experimental value of ~279 \AA^3 (Ross 1997; Zhang et al. 1997; Fiquet et al. 1994; Redfern et al. 1993). Therefore it is only meaningful to compare compression data normalized to its zero pressure value (i.e., V/V_0). The calculations (Fig. 2) show good agreement with Zhang et al. (1997) despite the discrepancy in the tabulated values of K_T and, in particular, $\partial K/\partial P$; the fitting parameters used in describing the equation of

TABLE 1. Calculated E-V data and pressure data from the third order Birch-Murnaghan equation

E (eV per formula unit)	V (\AA^3 per formula unit)	P (GPa)
-216.32189	295	-2.41596
-216.3758	285	0.877376
-216.316060	280	2.76545
-216.017602	270	7.1087
-215.759146	265	9.60368
-215.418504	260	12.3448
-213.046990	240	26.3528
-200.855027	200	78.6866
-167.715033	160	207.419

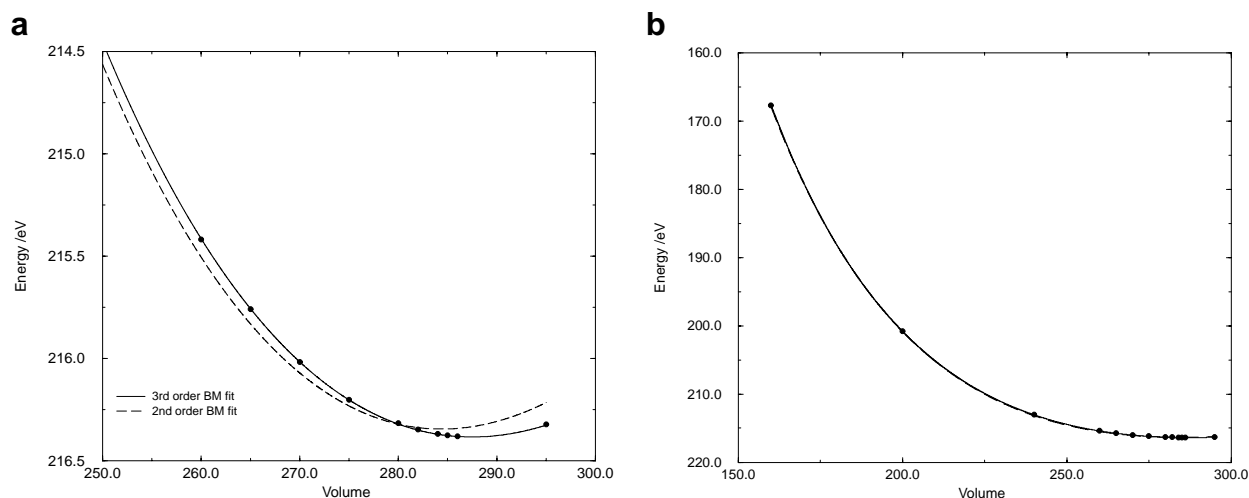
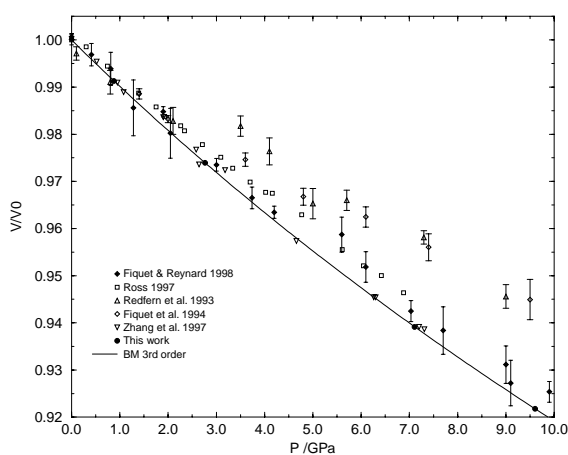


FIGURE 1. Energy vs. volume data fitted to both a second-order (dashed line) and third-order (full line) Birch-Murnaghan equation, (a) from 250–300 \AA^3 , and (b) 150–300 \AA^3 .

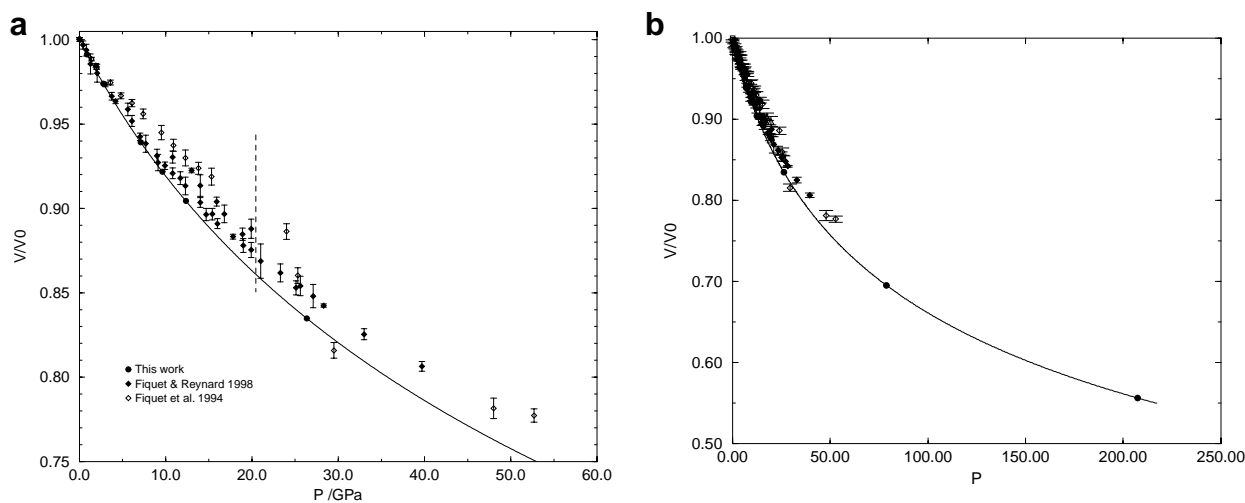
TABLE 2. Equation of state parameters from both theory and experiment

	Technique	$K_T(0)$ (GPa)	dK/dP
This Work	<i>Ab Initio</i> Simulations	99.0(5)	4.28(1)
Fiquet and Reynard (1998)	Powder XRD	111(1)	≈ 4
		108(2)	4.6(2)
Ross (1997)	Single crystal XRD	115	≈ 4
		117(3)	2.3(7)
Zhang et al. (1997)	Powder XRD	111(1)	≈ 4
		108(3)	2.3
Fiquet et al. (1994)	Powder XRD	103(1)	≈ 4
		156(4)	2.5(2)
Redfern et al. (1993)	Powder XRD	138(3)	≈ 4
		151(7)	2.5
Christensen (1972)	Ultrasonic	142(9)	≈ 4
		112*	—
Humbert and Plicque (1972)	Ultrasonic	113.8*	—

* Adiabatic bulk moduli.

**FIGURE 2.** Volumetric compression as a function of pressure in the range 0–10 GPa with a third-order Birch-Murnahan fit for $\partial K/\partial P = 4.28$ through the simulation results (filled circles). Where there are no error bars, experimental errors are within the data points.

state, in particular $K_T(0)$ and $\partial K/\partial P$, are known to be interdependent. No such agreement with the earlier work of Redfern et al. (1993) or Fiquet et al. (1994) exists; interestingly, however, the higher pressure data of a second series of experiments (16–53 GPa) of Fiquet et al. (1994), which they associate with a possible phase transition, appears in better agreement with the calculations (Fig. 3) where the discontinuity in compression serves to bring the data closer to the calculated equation of state. The calculated compression of the a and c axes (Fig. 4) are also in good agreement with the experimental data of Zhang et al. (1997) and also with Ross (1997), but in poor agreement with the earlier work of Redfern et al. (1993) and Fiquet et al. (1994). The calculated linear compressibilities are consistent with the experimental observation that the c axis is approximately 2.5 times as compressible as the a axis. Within the experimental range of pressures, the calculations give linear compressibilities of $1.73 \times 10^{-3} \text{ GPa}^{-1}$ for the a axis and $4.34 \times 10^{-3} \text{ GPa}^{-1}$ for the c axis. This compares with the experimental values of $1.88 \times 10^{-3} \text{ GPa}^{-1}$ and $4.22 \times 10^{-3} \text{ GPa}^{-1}$ (Ross 1997), $2.08 \times 10^{-3} \text{ GPa}^{-1}$ and $4.45 \times 10^{-3} \text{ GPa}^{-1}$ (Zhang et al. 1997) for the a and c axes respectively.

**FIGURE 3.** Volumetric compression as a function of pressure (a) to 60 GPa, and (b) to >200 GPa, compared with the results of Fiquet et al. (1994) and Fiquet and Reynard (1998); two sets of experimental data are shown separated by the vertical dashed line.

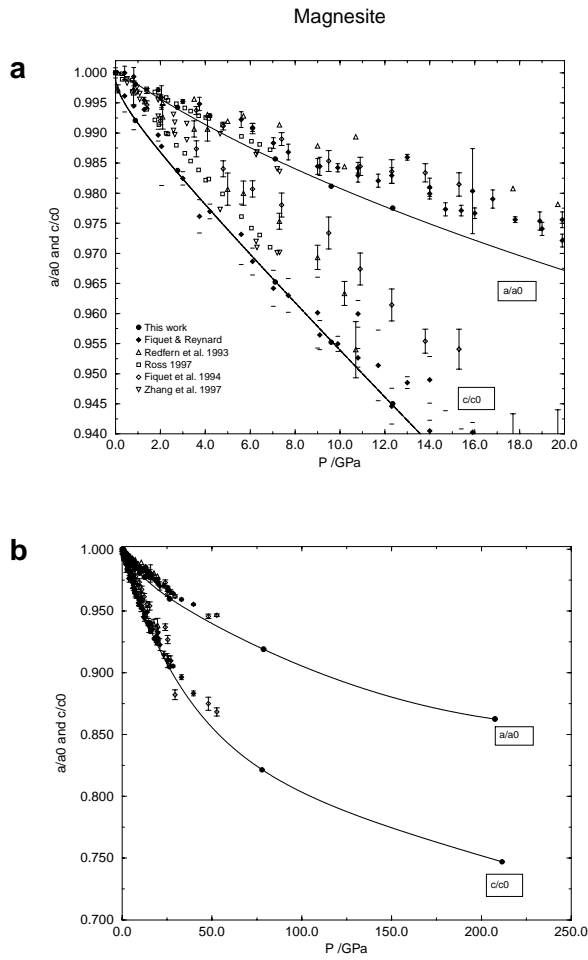


FIGURE 4. Axial compression as a function of pressures (a) from 0–20 GPa, and (b) to >200 GPa; the c axis is approximately 2.5 times as compressible as the a axis in the region 0–10 GPa.

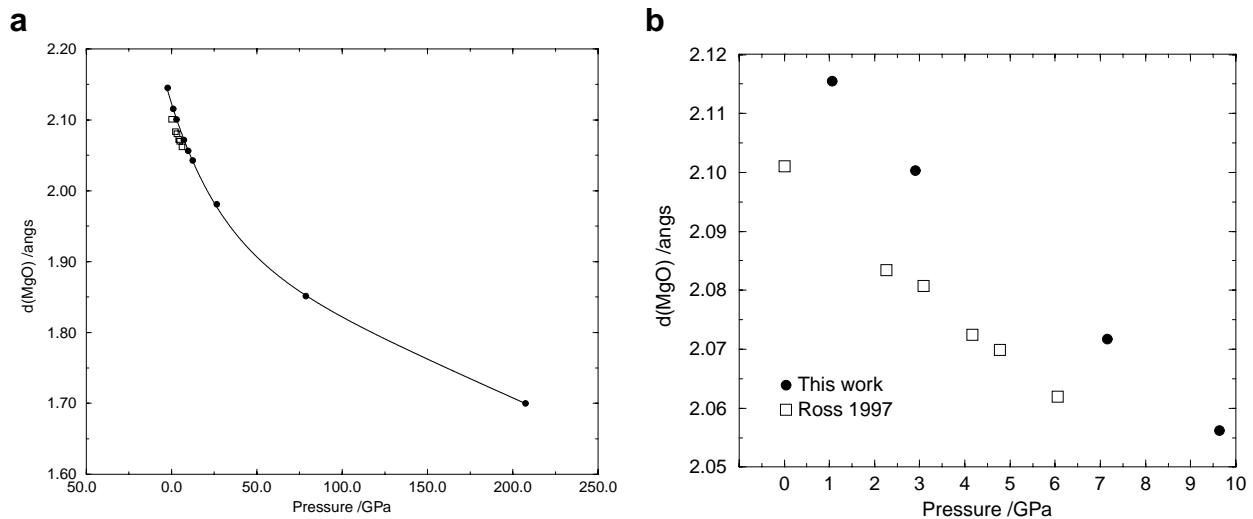


FIGURE 5. Calculated change in the Mg-O bond length as a function of pressure in the range (a) 0–200 GPa, and (b) 0–10 GPa, as compared with the experimental data of Ross (1997).

The simulations also predict details of the structural changes that magnesite undergoes with increasing pressure (up to 200 GPa). Magnesite consists of Mg atoms, which are surrounded by O atoms in octahedral coordination, layered between rigid CO_3 groups. Experiments of Ross (1997) show that the C-O bond length is highly incompressible between 0 and 7 GPa, whilst the Mg-O bond is significantly more compressible. These effects are also observed in the calculations (Figs. 5 and 6), and although the experimental results differ slightly from the calculated bond lengths in absolute values, due to the use of the GGA mentioned earlier, the linear compressibilities are in good agreement; the linear compressibility of the Mg-O bond is calculated to be $6.866 \times 10^{-3} \text{ GPa}^{-1}$ whereas that for the C-O bond is only $0.623 \times 10^{-3} \text{ GPa}^{-1}$. This compares well with the experimentally determined values of $6.384 \times 10^{-3} \text{ GPa}^{-1}$ and $0.857 \times 10^{-3} \text{ GPa}^{-1}$ for the Mg-O and C-O bond lengths respectively (Ross 1997).

The fully relaxed calculations show no obvious discontinuities in internal structure through either the compression mechanism or discontinuous changes in bond lengths. Over the entire pressure range studied (>200 GPa), the compression curves were smooth and continuous in all cases. Therefore the simulations show no evidence for any high pressure phase transition within the pressure range of the lower mantle. It is therefore probable that magnesite is stable throughout the lower mantle pressure range. It is possible that magnesite could be destabilized by temperature effects via some decarbonation reaction occurring at high pressure and temperature. However, recent high-pressure/high-temperature experiments (Zhang et al. 1997; Gillet 1993) and thermodynamic analysis of phase equilibria (Redfern et al. 1993) indicate that magnesite would remain stable in the uppermost part of the lower mantle. However, it must be emphasized that any type of phase transition involving an energy barrier would not be observed in these calculations, so the possibility of, for example, a reconstructive phase transition may not be ruled out.

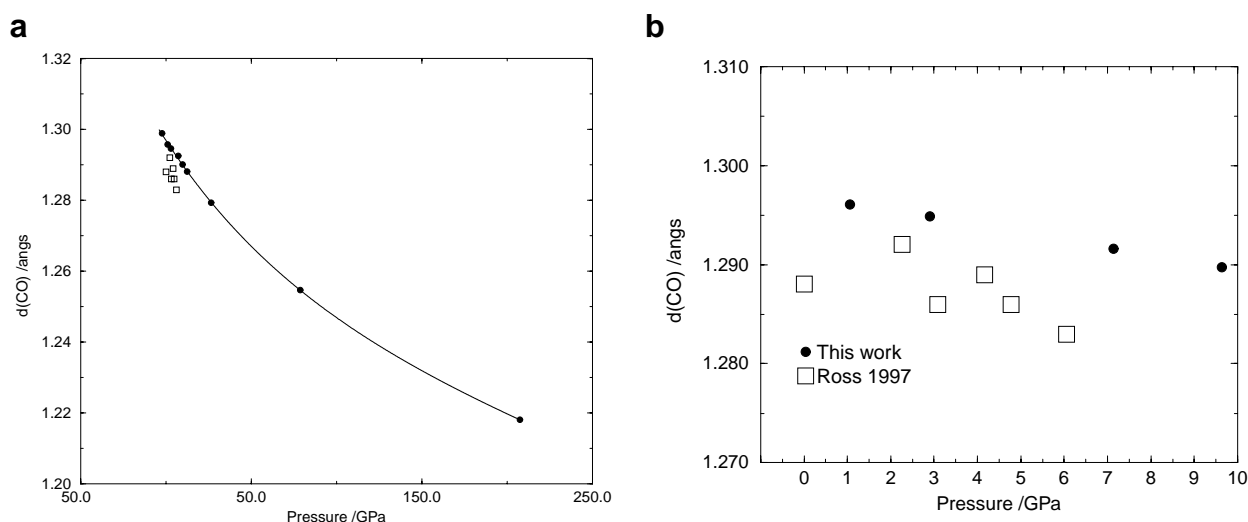


FIGURE 6. Calculated change in the C-O bond length as a function of pressure in the range (a) 0–200 GPa, and (b) 0–10 GPa, as compared with the experimental data of Ross (1997).

ACKNOWLEDGMENTS

I thank Nancy Ross, Ian Wood, and John Brodholt for constructive comments and discussion.

REFERENCES CITED

- Biellmann, C., Gillet, P., Guyot, F., Peyronneau, J., and Reynard, B. (1993) Experimental evidence for carbonate stability in the Earth's lower mantle. *Earth and Planetary Science Letters*, 118, 31–41.
- Brey, G., Brice, W.R., Ellis, D.J., Green, D.H., Harris, K.L., and Ryabchikov, I.D. (1983) Pyroxene-carbonate reactions in the upper mantle. *Earth and Planetary Science Letters*, 62, 64–74.
- Canil, D. and Scarfe, C.M. (1990) Phase relations in peridotite + CO₂ systems at 12 GPa: implications for origin of kimberlite and carbonate stability in the Earth's upper mantle. *Journal of Geophysical Research*, 95, 15805–15816.
- Christensen, N.I. (1972) Elastic properties of polycrystalline magnesium, iron and manganese carbonates to 10 kilobars. *Journal of Geophysical Research*, 77, 369–372.
- Eggler, D.H., Kushiro, I., and Holloway, J.R. (1976) Stability of Carbonate minerals in a hydrous mantle. *Carnegie Institution of Washington, Year Book* 75, 631–636.
- Fiquet, G. and Reynard, B. (1999) High pressure equation of state of magnesite: new data and a reappraisal. *American Mineralogist*, 84, 856–860.
- Fiquet, G., Guyot, F., and Itié, J.P. (1994) High pressure X-ray diffraction study of carbonates: MgCO₃, CaMg(CO₃)₂ and CaCO₃. *American Mineralogist*, 79, 15–23.
- Gillet, P. (1993) Stability of magnesite (MgCO₃) at mantle pressure and temperature conditions: a Raman spectroscopic study. *American Mineralogist*, 78, 1328–1331.
- Humbert, P. and Plicque, F. (1972) Propriétés élastiques des carbonates rhomboédriques monocristallins: calcite, magnésite et dolomie. *Comptes Rendus de l'Académie des Sciences de Paris*, 275, 391–394.
- Katsura, T., Tsuchida, Y., Ito, E., Yagi, T., Utsumi, W., and Akimoto, S. (1991) Stability of magnesite under lower mantle conditions. *Proceedings of the Japanese Academy*, 67, 57–60.
- Kresse, G. and Furthmüller, J. (1996) Efficient iterative schemes for ab initio total energy calculations using plane wave basis set. *Physical Review B*, 54, 11169–11186.
- Kresse, G. and Hafner, J. (1994) Norm conserving and ultrasoft pseudopotentials for first row elements and transition metals. *Journal of Physics: Condensed Matter*, 6, 8245–8257.
- Poirier, J.P. (1991) *Introduction to the physics of the Earth's interior*. Cambridge University Press.
- Redfern, S.A.T., Wood, B.J., and Henderson, C.M.B. (1993) Static compressibility of magnesite to 20 GPa: implications for MgCO₃ in the lower mantle. *Geophysical Research Letters*, 20, 2099–2102.
- Ross, N.L. (1997) The equation of state and high pressure behaviour of magnesite. *American Mineralogist*, 82, 682–688.
- Vanderbilt, D. (1990) Soft self-consistent pseudopotentials in a generalized eigenvalue formalism. *Physical Review*, B41, 7892–7895.
- Vocadlo, L., de Wijs, G., Kresse, G., Gillan, M., and Price, G.D. (1997) First principles calculations on crystalline and liquid iron at Earth's core conditions. *Faraday Discussions*, 106, 205–217.
- Vocadlo, L., Price, G.D., and Wood, I.G. (1999) Crystal structure and possible phase transitions in FeSi studied by first-principles pseudopotential calculations. *Acta Crystallographica*, in press.
- Wentzcovitch, R.M., Ross, N.L., and Price, G.D. (1995) Ab initio study of MgSiO₃ and CaSiO₃ perovskites at lower mantle pressures. *Physics of the Earth and Planetary Interiors*, 90, 101–112.
- Williams, Q., Collerson, B., and Knittle, E. (1992) Vibrational spectra of magnesite (MgCO₃) and calcite III at high pressures. *American Mineralogist*, 77, 1158–1165.
- Zhang, J., Martinez, I., Guyot, F., Gillet, P., and Saxena, S.K. (1997) X-ray diffraction study of magnesite at high pressure and high temperature. *Physics and Chemistry of Minerals*, 24, 122–130.

MANUSCRIPT RECEIVED NOVEMBER 3, 1998

MANUSCRIPT ACCEPTED JUNE 7, 1999

PAPER HANDLED BY LARS STIXRUDE